JACS
JOURNAL OF THE AMERICAN CHEMICAL SOCIETY
Article
pubs.acs.org/JACS

SSZ-87: A Borosilicate Zeolite with Unusually Flexible 10-Ring Pore Openings

Stef Smeets,[†] Lynne B. McCusker,*[,†] Christian Baerlocher,[†] Dan Xie,[‡] Cong-Yan Chen,[‡] and Stacey I. Zones*[,‡]

[†]Laboratory of Crystallography, ETH Zurich, Vladimir-Prelog-Weg 5, Zurich CH-8093, Switzerland
[‡]Chevron Energy Technology Company, Richmond, California 94802, United States

Supporting Information

ABSTRACT: The structure of the as-synthesized borosilicate zeolite SSZ-87 has been solved by combining high-resolution X-ray powder diffraction (XPD) and rotation electron diffraction (RED) techniques. The unit cell and space group symmetry were found from the XPD data, and were essential for the initial analysis of the RED data. Although the RED data were only 15% complete, this proved to be enough for structure solution with the program *Focus*. The framework topology is the same as that of ITQ-52 (**IFW**), but for SSZ-87 the locations of the structure directing agent (SDA) and the B atoms could also be determined. SSZ-87 has large cages interconnected by 8- and 10-rings. However, results of hydroisomerization and Al insertion experiments are much more in line with those found for 12-ring zeolites. This prompted the structure analyses of SSZ-87 after calcination, and Al insertion. During calcination, the material is also partially deboronated, and the location of the resulting vacancies is consistent with those of the B atoms in the as-synthesized material. After Al insertion, SSZ-87 was found to contain almost no B and to be defect free. In its calcined and deboronated form, the pore system of SSZ-87 is more flexible than those of other 10-ring zeolites. This can be explained by the fact that the large cages in SSZ-87 are connected via single rather than double 10-ring windows and that there are vacancies in some of these 10-rings.

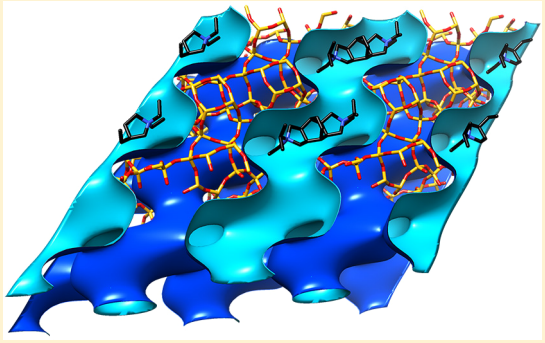

INTRODUCTION

Recently we described a new synthesis approach for silica-based zeolites using boric acid and ammonium fluoride to yield an alkali-free synthesis system. Both boron and fluoride became part of the synthesis product.[1] Two themes that emerged from the study were that products rich in boron could be made, and that the selectivity for the given zeolite product was often different from that of the zeolite synthesized using conventional sodium-borate-based reactions. By combining this new chemistry with a novel structure directing agent (SDA, Figure 1), the new zeolite SSZ-87 was produced.[2] The same SDA produced the known zeolite ZSM-12 (**MTW** framework type[3]) in the sodium-borate system. In this report we describe our attempts to understand the adsorption and catalytic properties of this new zeolite, and the solution of its structure using a combination of rotation electron diffraction and X-ray powder diffraction techniques.

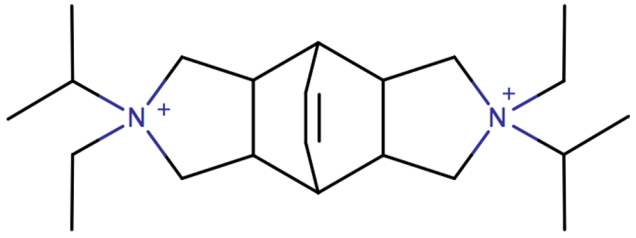

Figure 1. *N*,*N*′-Diisopropyl-*N*,*N*′-diethylbicyclo[2.2.2]oct-7-ene-2,3:5,6-dipyrrolidinium dication that was used as a structure directing agent in the synthesis of SSZ-87.

EXPERIMENTAL SECTION

Synthesis of Organic Structure Directing Agent. The *N*,*N*′-diisopropyl-*N*,*N*′-diethylbicyclo[2.2.2]oct-7-ene-2,3:5,6-dipyrrolidinium dication can be synthesized from bicyclo[2.2.2]oct-7-ene-2,3:5,6-tetracarboxylic dianhydride, which is a commercially available material. The dianhydride is initially reacted with isopropylamine to produce the bicyclo *N*,*N*′-disopropyl diimide which is then reduced with $LiAlH_4$ to produce the diamine. The diamine can then be alkylated with an ethyl halide (e.g., iodoethane) to produce the *N*,*N*′-diisopropyl-*N*,*N*′-diethyl quaternary dication.[4] To convert the diiodide salt to the hydroxide form, 3 g was dissolved in 15 mL of water. Then, 6 g of BioRad AG1-X8 hydroxide exchange resin was added and the mixure stirred at room temperature overnight. The solution was filtered free from the resin. Then, 3 mL of water was added to the resin and left standing for half an hour. The washing was collected again by filtration, and the two solutions were combined and titrated to give the OH molarity needed for the SSZ-87 synthesis.

Received: December 5, 2014

DOI: 10.1021/ja512411b
J. Am. Chem. Soc. XXXX, XXX, XXX−XXX

Synthesis of Borosilicate SSZ-87. A 4.5 mmol portion of *N*,*N*′-diisopropyl-*N*,*N*′-diethylbicyclo[2.2.2]oct-7-ene-2,3:5,6-dipyrrolidinium dihydroxide and 14 mmol of tetraethyl orthosilicate were added to a Teflon container. Next, 1 mmol of boric acid and 4.5 mmol of ammonium fluoride were added, and the mixture was allowed to stand in a closed configuration. After 2 days, the top was opened, and ethanol was allowed to evaporate. The H_2O/SiO_2 molar ratio was then adjusted to 20, and the Teflon liner was capped and sealed within a steel Parr autoclave. The autoclave was placed on a spit within a convection oven at 160 °C, where the autoclave was tumbled at 43 rpm over the course of 38 days. The autoclave was then removed from the oven and allowed to cool to room temperature. The solids were recovered by filtration and washed thoroughly with deionized water, and then allowed to dry at room temperature.

X-ray Powder Diffraction Data Collection. Synchrotron X-ray powder diffraction (XPD) data were collected on an as-synthesized sample of SSZ-87 in a 0.3 mm capillary on the Materials Science beamline at the Swiss Light Source (wavelength 1.0000 Å, MYTHEN II detector) in Villigen, Switzerland.[5]

Rotation Electron Diffraction Data Collection. Three-dimensional electron diffraction data sets were collected on six different crystals of as-synthesized SSZ-87 using the rotation electron diffraction (RED) technique.[6] The RED software was installed on a JEOL 2010 microscope operating at 200 kV, and data were collected over a tilt range of ±50° with a tilt step of 0.2° and an exposure time of 2 s. Relatively large tilt steps had to be used for these measurements, because the software to perform the finer tilts by tilting the electron beam had not yet been implemented. As a result, the RED data were not of optimal quality.

RESULTS

Characterization. The SSZ-87 sample proved to be stable to calcination, leaving an open structure with a micropore volume of nearly 0.17 cm^3/g as determined by N_2 adsorption, which is consistent with the size of the SDA used. Once the pores were open, we could apply a structural assessment tool that we devised recently for borosilicate zeolites. Al cations can replace B in the lattice if the pores are large enough to allow the hydrated Al cations to enter.[7] When this substitution occurs, the zeolite acquires acid sites strong enough to catalyze a variety of hydrocarbon transformation reactions. As the replacement takes place, a drop in the pH of the solution can be observed. Table 1 shows the pH drop and the Al uptake found for some comparatively open materials of known structure and for SSZ-87. The latter appears to be most similar to SSZ-33 (**CON**), which has a 3-dimensional channel system delimited by 12- and 10-ring pore openings.

Table 1. pH after Insertion of Al into Borosilicate Zeolites

zeolite	final pH[a] 96 h, 95 °C	wt % Al after 96 h, 95 °C
ZSM-11 (**MEL**)	3.00	0.01
SSZ-57 (***SFV**)	2.24	0.30
SSZ-33 (**CON**)	1.36	1.10
SSZ-87 (**IFW**)	1.44	0.95

[a]Initial pH = 3.

A useful assessment of a novel zeolite, when the crystal structure has not yet been determined, is the use of the isomerization of *n*-hexane by the Pd-loaded zeolite as a probe of its shape selectivity. In this test reaction, *n*-hexane is isomerized to bulkier products like methylpentanes and dimethylbutanes, the latter having the most difficulty in exiting the pores if there are restrictions.[8] Table 2 shows the values obtained for SSZ-87 in this test along with those for a number of other zeolites, some with restricted 10-ring apertures and some with 12-ring openings. ZSM-5 (**MFI**) is a classic intermediate pore (10-ring) zeolite, and one can see that the product selectivity is limited for the dimethylbutanes. The product distribution for SSZ-87, on the other hand, is much more in line with the 12-ring (large pore) zeolites such as ZSM-12 (**MTW**).

Table 2. Hydroisomerization and Hydrocracking of *n*-Hexane on Various Pd/Zeolites at Maximum Isomer Yield[a]

max isomer yield			distribution, mol %			
zeolite	temp, °C	mol %	2,2-DMBu	2,3-DMBu	2-MPn	3-MPn
Largest Pore Opening: 10-Ring						
ZSM-5	260	74.4	0.2	3.0	59.6	37.2
SSZ-32	304	68.5	0.1	2.1	58.9	38.9
SSZ-75	254	63.8	0.6	9.1	55.0	35.3
TNU-9	260	77.4	2.6	13.1	51.8	32.5
SSZ-25	271	74.5	0.5	5.1	57.3	37.1
Largest Pore Opening: 12-Ring						
SSZ-57	260	76.3	3.2	9.9	54.0	32.9
SSZ-56	266	65.3	6.4	9.4	50.9	33.3
SSZ-26	260	78.8	9.9	12.8	47.0	30.3
SSZ-33	271	79.1	11.9	12.4	46.0	29.7
ZSM-12	260	72.7	16.2	9.6	44.8	29.4
MOR	293	78.6	21.5	10.8	40.7	27.0
Y	304	79.5	21.9	10.0	41.1	27.0
SSZ-87	349	68.7	14.2	9.2	45.6	31.0
Therm. equilib.	277		37.8	18.5	30.6	13.1

[a]DMBu, dimethylbutane; MPn, methylpentane.

The final indirect measurement we performed to characterize the pore system of SSZ-87 was the adsorptive uptake of 2,2-dimethylbutane.[9] Large pore zeolites rapidly admit this roughly 6 Å cross-section adsorbate, while intermediate pore zeolites like ZSM-5 admit it only slowly. The uptake curves for several different zeolites are shown in Figure 2. SSZ-87 does not show the same behavior as the large pore zeolites, but the initial filling is more rapid than for ZSM-5. The uptake then levels off and is much more gradual, yielding a profile higher but parallel to that of ZSM-5. There appears to be some barrier to the total free uptake of 2,2-dimethylbutane in SSZ-87.

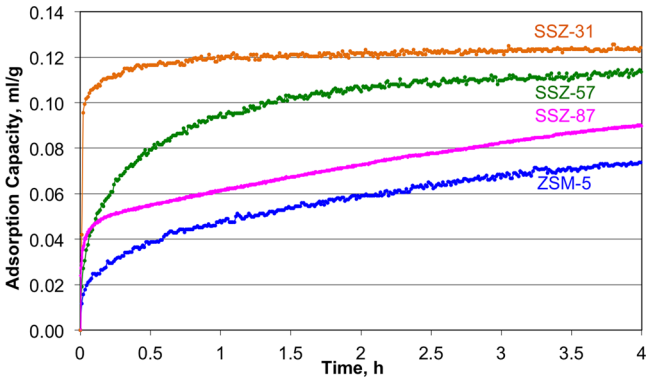

Figure 2. 2,2-Dimethylbutane adsorption in various zeolites.

Structure Analysis of As-Synthesized SSZ-87. While the measurements described above were in progress, attempts were being made to determine the structure of this new zeolite. The XPD pattern could be indexed with a monoclinic *C*-centered unit cell (*C*2, *Cm*, or *C*2/*m*; a = 21.21 Å, b = 17.84 Å, c = 12.30 Å, β = 124.75°) using the indexing routine in the program

DOI: 10.1021/ja512411b
J. Am. Chem. Soc. XXXX, XXX, XXX−XXX

TOPAS.[10] This was followed by intensity extraction using the Pawley[11] profile-fitting routine implemented in the same program.[12] Structure determination was attempted in all three space groups, both with the zeolite-specific structure solution program *Focus*[13] and with the powder charge flipping algorithm (*pCF*)[14] implemented in the program *Superflip*[15] using optimized input parameters,[16] but no interpretable solutions could be identified.

Therefore, we turned to the RED data, even though the data sets were not ideal. Eventually, after considerable effort, one of the six patterns could be indexed with a triclinic unit cell using the RED software,[18] but it did not seem to be consistent with the XPD data. Typically, unit cells derived from electron diffraction data have an error of up to 1.0%, so the LePage algorithm implemented in the program *PLATON*[19] was used to search for higher symmetry. Only by using very high tolerances was it possible to identify an approximately monoclinic *C*-centered unit cell (a = 21.21 Å, b = 17.11 Å, c = 11.96 Å, α = 90.9°, β = 125.6°, γ = 90.3°) that resembled the unit cell from the XPD data. Although the reflection intensities extracted using this unit cell were only 15% complete (to a d-spacing of 1.2 Å), structure solution, assuming the space group $C2/m$, was attempted. For this, a version of *Focus* that had been adapted to accommodate electron diffraction data[20] was applied. The two top solutions occurred 218 and 109 times, respectively. A distance least-squares (DLS) refinement[21] showed both to be intrinsically feasible, so preliminary refinements using the Rietveld method[22] were performed. The most frequently occurring solution proved to be the correct one. More details of the structure solution are given in Table 3.

Table 3. Details of the Solution of the Structure of As-Synthesized SSZ-87 Using *Focus* with RED Data[a]

reflns measured	444
unique reflns	177
reflns used	177
d_{min} (Å) of reflns used	1.21
completeness[b]	15%
trials	40 000
correct solutions	218
total CPU time (h)	1.6
sec/correct solution	27

[a]The computations were performed in parallel on a 2010 Mac Pro equipped with dual 2.4 GHz Quad-Core Intel Xeon processors. [b]Completeness of the full data set up to d_{min} corresponding to the reflections used.

Once the correct framework had been identified (Figure 3a), geometric restraints were applied to all unique bond distances and angles. An approximate scale factor was determined by performing a few cycles of refinement with just the higher angle XPD data, keeping all other parameters fixed. Then, a difference electron density map, generated using this scale factor with the whole pattern, revealed an electron cloud in the zeolite pores with the approximate shape of the SDA (Supporting Information Figure S8). An initial model for the SDA was created and optimized using the energy minimization routine in *Jmol*.[23] The molecule was added to the structural model as a rigid body, and its location and orientation were optimized using the simulated annealing routine in *TOPAS*. In this process, the SDA settled on a position with 4-fold disorder (2/m) in the center of the cage. After a few cycles of refinement, it

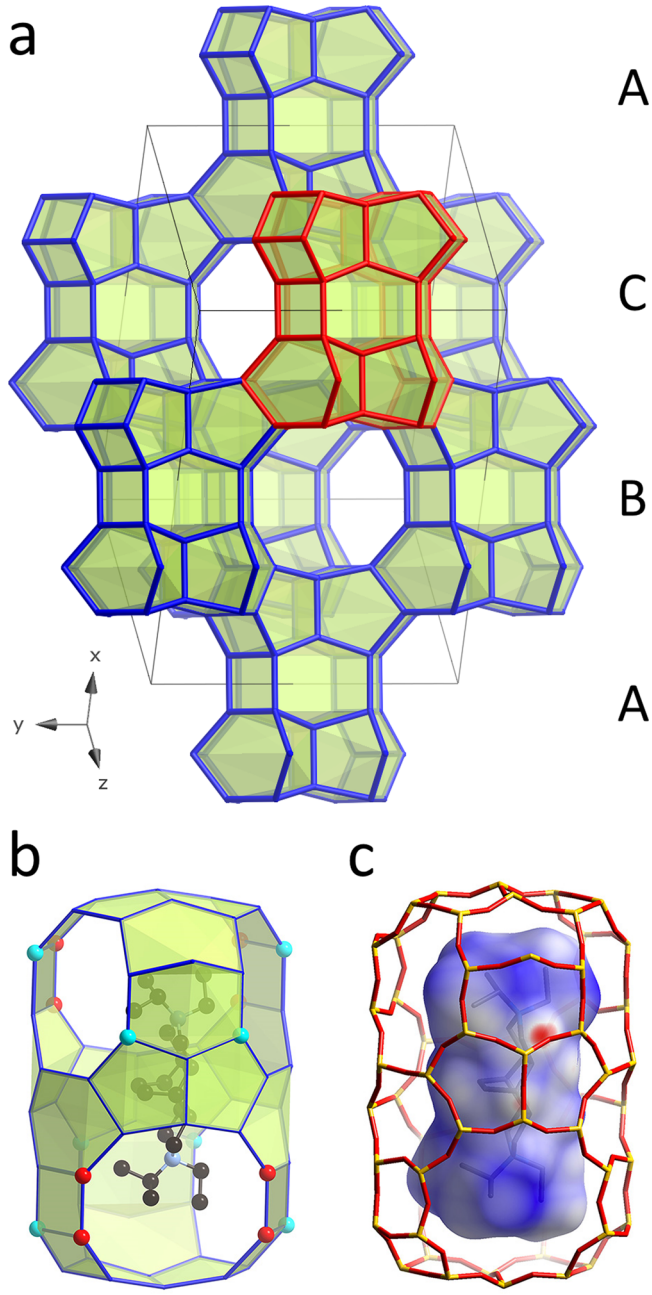

Figure 3. Framework structure of as-synthesized SSZ-87. (a) The ABC-type stacking of the building block given in red, (b) the large [$10^2 8^4 6^8 5^8 4^8$] cavity showing the refined position of the SDA and the location of the two T sites containing B (red, T7; cyan, T8), and (c) the cavity showing the Hirshfeld surface[17] of the SDA. Bridging O atoms in parts a and b have been omitted for clarity.

aligned itself along the 2-fold axis, so it was placed on the axis, thereby reducing the disorder by a factor of 2, and the rigid body description was replaced with a geometrically restrained model. H atoms were added in their geometrically expected positions for the final stages of refinement.

It was not clear from the synthesis procedure which configuration the SDA would adopt, so a quick analysis of a single crystal of the pure material was performed to remove this ambiguity. It was found to cocrystallize with water in space group $P2_1/n$, with 4 SDA molecules per unit cell (a = 9.5974(6) Å, b = 16.103(2) Å, c = 14.9912(17) Å, β = 89.746(8)°). Although the crystal was small, the data were good

DOI: 10.1021/ja512411b
J. Am. Chem. Soc. XXXX, XXX, XXX−XXX

enough to determine the configuration of the SDA. It has 2-fold symmetry with the terminal isopropyl groups in a *cis* configuration.

By introducing an anisotropic peak broadening model,[24] the profile fit could be improved significantly. All atomic positions were refined with isotropic displacement parameters and by using scattering factors for neutral atoms. The final difference electron density map was essentially featureless. Details of the refinement are given in Table 4, and the profile fit is shown in Figure 4.

Table 4. Crystallographic Data for As-Synthesized SSZ-87

chemical composition	$\mathrm{I(C_{22}H_{40}N_2)_2I[Si_{60}B_4O_{128}]}$
space group	*C*2/*m*
a (Å)	21.1727(5)
b (Å)	17.8092(5)
c (Å)	12.2869(2)
β (deg)	124.8(1)
V (Å^3)	3804.7(2)
2*θ* range (deg)	3.1−60.0
λ (Å)	0.999 90(1)
R_I	0.037
R_{wp}	0.103
R_{exp}	0.010
GOF	10.0
observations	15 135
reflns	2123
params	193
geometric restraints	210

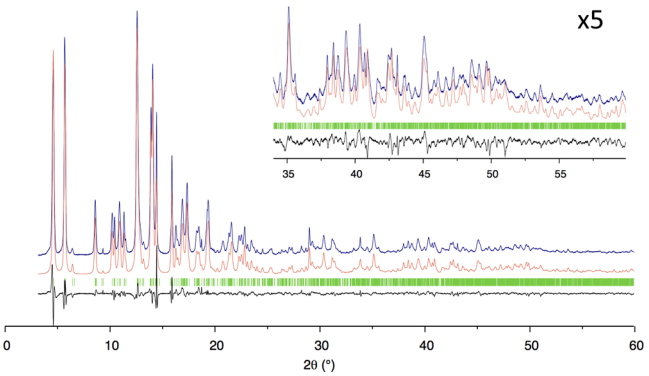

Figure 4. Observed (blue), calculated (red), and difference (black) profiles for the Rietveld refinement of SSZ-87. The high angle data shown in the inset have been scaled up by a factor of 5 to show more detail.

Up to this point, all tetrahedrally coordinated atoms (T atoms) in the SSZ-87 framework structure had been treated as Si atoms. In order to find the B atoms, the T atom positions were redefined as mixed Si/B positions with a total occupancy of 1. Only the positions T7 and T8 refined with a significant amount of B (0.19 and 0.31, respectively, Figure 3b). All the others refined close to 1 Si and 0 B, so they were reset to 100% Si, and the geometric restraints for T7 and T8 were adjusted to reflect the shorter B−O distance (using a weighted linear combination of 1.48 Å for B−O and 1.61 Å for Si−O). In the final cycles of refinement, the occupancies of these two positions refined to 0.849 Si (0.151 B) and 0.646 Si (0.354 B), respectively.

DISCUSSION

Structure. The framework structure of SSZ-87 can be viewed as an ordered ABC-type stacking of an *rte* composite building unit[25] surrounded by four $[4^3 5^4 6^1]$ cages to create the framework shown in Figure 3b with large $[10^2 8^4 6^8 5^8 4^8]$ cavities in between the units (Figure 3c). The cavity can be described as a prolate spheroid with free dimensions of 15.34 Å × 7.41 Å × 7.15 Å and an effective volume of ca. 290 Å^3. The long axis of the cavity is aligned with the $[10\bar{1}]$ direction, and the next cavity is shifted along this vector by half a cavity length in a staircase-like arrangement. Each cavity is connected to the two neighboring ones via shared 10-rings to form straight 10-ring channels running parallel to the *z*-axis (Figure 5). The effective

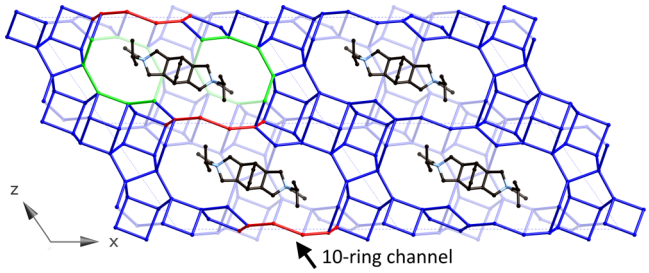

Figure 5. Projection of the structure of SSZ-87 along [010] showing the arrangement of the large cavities and the SDA. The 10-rings of one channel along the [001] direction have been highlighted in red, and the 8-rings along [010] for one cavity in green. The top layer has been removed to show the cavities more clearly. Bridging O atoms have been omitted for clarity.

pore opening for this 10-ring channel is 4.99 Å × 5.54 Å. Each cavity is further connected to four more cavities along the [010] direction via shared 8-rings to form a 3-dimensional channel system.

The SDA fits the large cavity very well. This is well-illustrated by the Hirshfeld surface[17] (Figure 3c). The color scheme used on this surface indicates the contact distances to the framework. Where the contacts are about equal to the sum of the van der Waals radii, the surface is colored white, short contacts are highlighted in red, and long ones in blue. The shortest C···O distance is 3.28 Å, between C5 and O13 (Supporting Information), and is visualized by the red spot on the Hirshfeld surface. All other distances are over 3.6 Å. In the refined structure, the cation is disordered over two positions that are related by a mirror plane. That is, it can adopt either position (isopropyl groups pointing up or down) in any given unit cell. The two N atoms carrying the positive charge are located near the ends of the SDA, and these positions are near the location of the T sites containing B (Figure 3b). Furthermore, the total population of B atoms refined to 4.04 per unit cell, which correlates well with the number required to balance the charge of the two doubly charged cations per unit cell.

A very similar SDA, with ethyl groups in place of the isopropyl groups, was used in the synthesis of the pure-silica zeolite YNU-2b (**MSE**).[26] As in SSZ-87, the framework of YNU-2b is characterized by elongated cavities (effective dimensions 16.68 Å × 7.38 Å × 6.27 Å) that are interconnected by 12-ring channels, and accessible through 10-ring apertures. The SDA is centered in this cavity.

Recently, the synthesis and structure of the borosilicate zeolite ITQ-52 (**IFW**) was reported by the Corma group.[27] They were investigating the use of a new family of amino-

DOI: 10.1021/ja512411b
J. Am. Chem. Soc. XXXX, XXX, XXX−XXX

phosphonium cations as SDAs. Under certain conditions, the 1,4-butanediyl bis[tris(dimethylamino)]phosphonium dication led to the formation of ITQ-52. The framework structure of ITQ-52 was determined using *Focus* on synchrotron XPD data collected on a calcined sample. We were most surprised to discover that the framework structure of SSZ-87 is identical to that of ITQ-52. Because the ITQ-52 structure was determined from data collected on a calcined sample, the location of the SDA was not reported, but a comparison of the ITQ-52 and SSZ-87 SDAs shows that the distance between the charged atoms in the two dications is quite similar (Figure 6). The

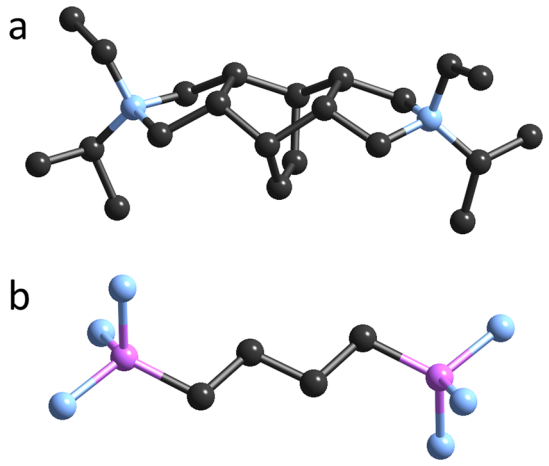

Figure 6. Comparison of the SDAs used to synthesize (a) SSZ-87 ($(C_2H_5)(C_3H_7)NC_{12}H_{16}N(C_2H_5)(C_3H_7)$) and (b) ITQ-52 ($(NH_2)_3P(CH_2)_4P(NH_2)_3$). H atoms have been omitted for clarity.

positions of the B atoms in the framework structure of ITQ-52 were not determined, but the B content is comparable to that of SSZ-87, so we expect that the B atoms occupy similar positions in ITQ-52.

Al insertion. Recent Al insertion experiments showed that Al can replace B when B is in a 12- or larger ring.[7] Much to our surprise, after Al insertion tests on calcined SSZ-87 nearly all B atoms are replaced by Al atoms (Supporting Information Table S5). As in the hydroisomerization characterization experiment, this is much more consistent with a large pore zeolite than with an intermediate pore one. To better understand this finding, the structures of a sample after calcination, and of a sample after Al insertion were analyzed (Supporting Information). In both cases, the framework structure was found to be very similar to that of the as-synthesized material, and no significant differences in pore diameter could be discerned.

From the NMR data, it is clear that only about half of the B was removed from the SSZ-87 framework upon calcination. T atom occupancy refinement showed that all T atom sites except T8 were occupied predominantly by Si. T8 refined to 0.623 Si. By taking the information from the NMR experiments into account in the XPD structure refinement, T8 could be assigned a Si:B:vacancy ratio of approximately 0.5:0.3:0.2. This is in line with the B assignment in the structure analysis of the as-synthesized SSZ-87 material. The presence of vacancies might explain why the hydroisomerization and Al insertion results are more indicative of a large pore than an intermediate pore opening.

Structure refinement shows that all T sites are fully occupied after the Al insertion. Although the distribution of Al in the framework could not be determined, we expect the Al to occupy primarily the T8 and perhaps the T7 sites. In view of the fact that the Si:Al ratio of 40 is higher than the initial Si:B ratio of 15, we suspect that Si is also acting as a "healing agent" during the Al insertion.[28,29] The B content of the aluminated material is lower than that of the calcined material, so it appears that Al or Si replace B, whether it was removed from the framework in a previous step or not.

Internal flexibility of SSZ-87. The effective pore opening of the 10-ring in SSZ-87 lies within the range of those of the five other 10-ring zeolites examined for comparison (Supporting Information Table S6). These all behave differently from SSZ-87 in the isomerization of *n*-hexane tests (Table 2), so there must be some kind of intrinsic structural flexibility that allows the large 2,2-dimethylbutane molecule to wriggle its way through the SSZ-87 pores. The unique feature of SSZ-87 is that it consists of large cages delimited by a 14-ring in the middle, interconnected by single 10-ring windows. It may be that, because the 10-rings are single, the O atoms can be displaced more easily, and because the cages are large, a bulky organic molecule can orient itself more freely to wend its way through the restriction. This flexibility is then further enhanced by the presence of defects in the 10-ring. Although both ZSM-5 (**MFI**) and TNU-9 (**TUN**) have 3-dimensional channel systems with pore openings slightly larger than those of SSZ-87, their 10-ring openings are reinforced by a second 10-ring connected directly to the first, and this significantly reduces the flexibility of the opening. Even if vacancies are present, the reinforcing 10-ring limits their effect on the effective pore opening. SSZ-75 (**STI**) and SSZ-32 (**MTT**) both have straight channels with pore openings smaller than those of SSZ-87, and no large pockets or cages. SSZ-25 (**MWW**) does have large side pockets between the layers, but the pores to access them are elliptical and much smaller than those of SSZ-87.

■ CONCLUSIONS

The structure of SSZ-87 has been solved from a combination of high quality powder diffraction and poor quality rotation electron diffraction data. The XPD data provided the unit cell and space group symmetry, and was essential for the initial interpretation of the RED data. Although the RED data set was only 15% complete, *Focus* proved to be powerful enough to deal with it. This is the second example where low quality RED data proved to be better suited for structure solution using *Focus* than high quality XPD data.[30]

The framework topology was found to be the same as that of ITQ-52, but for SSZ-87 it was possible to locate the SDA within the cage, as well as the positions of the B atoms in the framework. The location of the B atoms could be confirmed by a further structure analysis of a calcined sample.

In view of the results of hydroisomerization and Al insertion experiments, the pore system of SSZ-87 appears to be somewhat more flexible in its calcined form than other high-silica zeolites with 10-ring channel systems. This flexibility might be a result of the fact that the 10-rings in SSZ-87 are single ones that connect very large cages coupled with the presence of vacancies in some of these 10-rings. The result is a zeolite with characteristics that are intermediate between those of 10- and 12-ring pore zeolites.

■ ASSOCIATED CONTENT

Supporting Information

Results of ^{11}B and ^{29}Si NMR analyses, detailed information on the structure analyses of calcined and of aluminated SSZ-87

DOI: 10.1021/ja512411b
J. Am. Chem. Soc. XXXX, XXX, XXX−XXX

including Rietveld plots, elemental analysis, SEM image of as-synthesized SSZ-87, selected bond distances, and crystallographic data for (1) as-synthesized, (2) calcined and (3) aluminated SSZ-87 in CIF format. This material is available free of charge via the Internet at http://pubs.acs.org.

AUTHOR INFORMATION

Corresponding Authors

mccusker@mat.ethz.ch
sizo@chevron.com

Notes

The authors declare no competing financial interest.

ACKNOWLEDGMENTS

This work was supported by the Swiss National Science Foundation and the Chevron Energy Technology Company. We thank Nicola Casati for his assistance with the powder diffraction measurements on the Materials Science Beamline at the SLS in Villigen, Switzerland, Tom Rea at Chevron ETC for the RED data collection, and Son-Jong Hwang from Caltech for the NMR data collection. We also thank Lisa Gibson and Allen Burton for the synthesis of the SDA used here, while they were at Chevron ETC. Funding from the Swiss National Science Foundation is gratefully acknowledged.

REFERENCES

(1) Zones, S. I.; Hwang, S.-J. *Microporous Mesoporous Mater.* **2011**, *146*, 48.
(2) Zones, S. I. U.S. Patent 8,545,800, 2013.
(3) Three-letter framework type codes (boldface capital letters) for all zeolites mentioned in the text are given in parentheses. They can be found in Baerlocher, C.; McCusker, L. B.; Olson, D. H. *Atlas of Zeolite Framework Types*, 6th revised ed.; Elsevier: Amsterdam, 2007 or at http://www.iza-structure.org/databases/.
(4) Dhingra, S. S.; Weston, S. C. U.S. Patent 6,656,268, 2003.
(5) Bergamaschi, A.; Cervellino, A.; Dinapoli, R.; Gozzo, F.; Henrich, B.; Johnson, I.; Kraft, P.; Mozzanica, A.; Schmitt, B.; Shi, X. T. *J. Synchrotron Radiat.* **2010**, *17*, 653.
(6) Zhang, D.; Oleynikov, P.; Hovmöller, S.; Zou, X. D. *Z. Kristallogr.* **2010**, *225*, 94.
(7) Zones, S. I.; Benin, A.; Hwang, S.-J.; Xie, D.; Elomari, S. *J. Am. Chem. Soc.* **2014**, *136*, 1462.
(8) Chen, C. Y.; Ouyang, X.; Zones, S. I.; Banach, S. A.; Elomari, S. A.; Davis, T. M.; Ojo, A. F. *Microporous Mesoporous Mater.* **2012**, *104*, 71.
(9) Chen, C. Y.; Zones, S. I. *Microporous Mesoporous Mater.* **2007**, *164*, 39.
(10) Coelho, A. A. *J. Appl. Crystallogr.* **2003**, *36*, 86.
(11) Pawley, G. S. *J. Appl. Crystallogr.* **1981**, *14*, 357.
(12) Coelho, A. A. *TOPAS-ACADEMIC v4.1*; 2007.
(13) Grosse-Kunstleve, R. W.; McCusker, L. B.; Baerlocher, C. *J. Appl. Crystallogr.* **1997**, *30*, 985.
(14) Baerlocher, C.; McCusker, L. B.; Palatinus, L. *Z. Kristallogr.* **2007**, *222*, 47.
(15) Palatinus, L.; Chapuis, G. *J. Appl. Crystallogr.* **2007**, *40*, 786.
(16) Sisak, D.; Baerlocher, C.; McCusker, L. B.; Gilmore, C. J. *J. Appl. Crystallogr.* **2012**, *45*, 1125.
(17) Spackman, M. A.; Jayatilaka, D. *CrystEngComm* **2009**, *11*, 19.
(18) Wan, W.; Sun, J. L.; Su, J.; Hovmoller, S.; Zou, X. D. *J. Appl. Crystallogr.* **2013**, *46*, 1863.
(19) Spek, A. L. *J. Appl. Crystallogr.* **2003**, *36*, 7.
(20) Smeets, S.; McCusker, L. B.; Baerlocher, C.; Mugnaioli, E.; Kolb, U. *J. Appl. Crystallogr.* **2013**, *46*, 1017.
(21) Baerlocher, C.; Hepp, A.; Meier, W. M. *DLS-76, A Program for the Simulation of Crystal Structures by Geometric Refinement*; Institute of Crystallography and Petrography, ETH Zurich: Zurich, 1977.
(22) Rietveld, H. M. *J. Appl. Crystallogr.* **1969**, *2*, 65.
(23) Hanson, R. M. *J. Appl. Crystallogr.* **2010**, *43*, 1250.
(24) Stephens, P. W. *J. Appl. Crystallogr.* **1999**, *32*, 281.
(25) Baerlocher, C.; McCusker, L. B.; Olson, D. H. *Atlas of Zeolite Framework Types*; Elsevier: Amsterdam, 2007. Baerlocher, C.; McCusker, L. B. *Database of Zeolite Structures*; http://www.iza-structure.org/databases/.
(26) Koyama, Y.; Ikeda, T.; Tatsumi, T.; Kubota, Y. *Angew. Chem., Int. Ed.* **2008**, *47*, 1042.
(27) Simancas, R.; Jordá, J. L.; Rey, F.; Corma, A.; Cantín, A.; Peral, I.; Popescu, C. *J. Am. Chem. Soc.* **2014**, *136*, 3342.
(28) Jones, C. W.; Hwang, S.-J.; Okubo, T.; Davis, M. E. *Chem. Mater.* **2001**, *13*, 1041.
(29) Chen, C. Y.; Zones, S. I. *Zeolites and Catalysis—Synthesis, Reactions and Applications*; Čejka, J., Corma, A., Zones, S. I., Eds.; Wiley-VCH Verlag: New York, 2010; p 155.
(30) Smeets, S.; Xie, D.; McCusker, L. B.; Baerlocher, C.; Zones, S. I.; Thompson, J. A.; Lacheen, H. S.; Huang, H.-M. *Chem. Mater.* **2014**, *26*, 3909.

DOI: 10.1021/ja512411b
J. Am. Chem. Soc. XXXX, XXX, XXX−XXX